
Unsupervised Domain Alignment of Fingerprint Denoising Models using Pseudo Annotations

Indu Joshi^{1,2,*} · Tushar Prakash³ · Rohit Kumar³ · Antitzia Dantcheva¹ · Sumantra Dutta Roy² · Prem Kumar Kalra²

Received: date / Accepted: date

Abstract State-of-the-art fingerprint recognition systems perform far from satisfactory on noisy fingerprints. A fingerprint denoising algorithm is designed to eliminate noise from the input fingerprint and output a fingerprint image with improved clarity of ridges and valleys. To alleviate the unavailability of annotated data to train the fingerprint denoising model, state-of-the-art fingerprint denoising models generate synthetically distorted fingerprints and train the fingerprint denoising model on the synthetic data. However, a visible *domain shift* exists between synthetic training data and the real-world test data. Subsequently, state-of-the-art fingerprint denoising models suffer from poor generalization. To counter this drawback of state-of-the-art, this research proposes to align the synthetic and real fingerprint domains. Experiments conducted on publicly available rural Indian fingerprint demonstrate that after the proposed domain alignment, equal error rate improves from 7.30 to 6.10 on Bovzorth matcher and 5.96 to 5.31 on minutiae cylinder code (MCC) matcher. Similar improved fingerprint recognition results are obtained for IIITD-MOLF and private rural fingerprints database as well.

Keywords Fingerprint enhancement · Unsupervised domain adaptation · Self-supervision · Latent fingerprints

1 Introduction

Fingerprint recognition systems are among the most popular biometrics trait. These are frequently exploited in applications including border security, access control, and law enforcement. However, the performance of fingerprint recognition systems on

* indicates corresponding author- Indu Joshi: E-mail: indu.joshi@inria.fr

¹ Inria Sophia Antipolis, France

² Indian Institute of Technology Delhi, India

³ Delhi Technological University, India

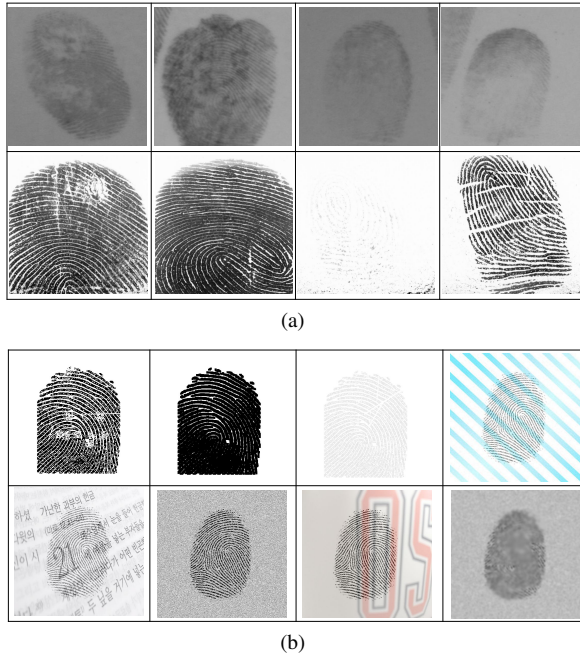


Fig. 1 (a) Sample examples of (real) fingerprints from the IIITD- MOLF Database [49] (top row), and the Rural Indian Fingerprint Database [44] (bottom row) (b) Sample training samples of synthetically distorted fingerprints. There is a visible *domain shift* between the synthetically distorted and real distorted fingerprints. Subsequently, existing fingerprint denoising models trained on the synthetic data lack generalization to real-world distorted fingerprints.

low quality fingerprints obtained for subjects involved in a high amount of manual labor and aged subjects is unsatisfactory [60,44,56]. Similarly, the fingerprint recognition performance on fingerprints obtained from a crime scene (latent fingerprints) is also poor. The challenge in poor quality live scan fingerprints arises due to the presence of scars, warts, dry or wet fingertips leading to unclear or thick ridges [22]. On the other hand, a latent fingerprint is characterized by smudged ridge patterns and complex backgrounds with lines, text, stains, and sometimes overlapping fingerprints (See Figure 1 (a)).

A fingerprint denoising model is designed to eliminate noise from a poor quality input fingerprint image and generate a higher quality fingerprint image with an enhanced ridge structure. Subsequently, improving the fingerprint comparison scores. State-of-the-art fingerprint denoising models are supervised models that are trained on pixel-level annotated data of poor quality distorted and the corresponding good quality enhanced image. However, there is no publicly available annotated training set available to train a fingerprint denoising model. To address this limitation on the availability of a pixel-level annotated dataset, researchers train the model on the synthetically distorted fingerprints instead [64,45]. The synthetically distorted fingerprints are generated by introducing different distortions such as Gaussian blurring, lines, blending with varying textures [23,35] (See Figure 1 (b)). However, as also

illustrated in Figure 1, there is a visible *domain shift* in real low quality and synthetically distorted fingerprints. As a result, state-of-the-art fingerprint denoising models are limited in their ability to generalize to real low quality fingerprints.

1.1 Research Contributions

To address this limitation of state-of-the-art fingerprint denoising models, this paper formulates fingerprint denoising as an *unsupervised domain adaptation* problem and proposes to align the source and target domains, i.e., synthetically distorted and real low quality fingerprints. In particular, we introduce two *auxiliary tasks* of predicting rotation and location for both annotated synthetically distorted fingerprints (source domain) and unannotated real poor quality fingerprints (target domain). The model jointly optimizes learning of fingerprint denoising as well the two auxiliary tasks. The introduction of these auxiliary tasks simultaneously on both the domains helps to align the representations learnt for both the domains and improve fingerprint denoising performance on the real fingerprints. The contributions of this paper are summarized as below:

- Impact of domain alignment of synthetic and real distorted fingerprints is studied. In particular, two auxiliary tasks of rotation and location prediction are introduced to bridge the domain gap between real and synthetic fingerprints.
- To the best of our knowledge, no study so far in the fingerprint denoising literature has exploited multi-task learning to align synthetic and real fingerprint domains.
- The proposed DA-GAN and the most recent fingerprint denoising models are thoroughly compared. Additionally, a comparison between the proposed DA-GAN and state-of-the-art fingerprint denoising models based on generative adversarial networks (GAN) is done.
- Ablation study illustrating the contribution of each auxiliary task in improving the fingerprint denoising performance is provided.
- A comprehensive analysis of successful and challenging cases for the proposed DA-GAN is presented.
- Improved fingerprint recognition performance on challenging latent fingerprints and fingerprints of the rural Indian population signifies improved generalization ability of the proposed DA-GAN.

1.2 Organization of Paper

Given the wide applications of fingerprint recognition technology, the main contribution of this research is to enhance the quality of noisy fingerprints and subsequently improve its recognition performance. Towards this, Section 2 provides a summary of the most *recent developments* in the field. Section 3 introduces the *proposed domain alignment* technique for fingerprint denoising, while Section 4 elaborates *implementation details*. Section 5 provides details on the *experimental protocols*. In Section 6, the effectiveness of the proposed DA-GAN is evaluated in *comparison* to the most recent *fingerprint denoising models*. Section 7 delves into providing insights on the

proposed model through *ablation studies* and *discussions* on challenging cases. Finally, Section 8 *concludes* the research findings and discusses future scope.

2 Related Work

2.1 Fingerprint Denoising

2.1.1 Denoising using Classical Image Processing Methods

The most widely used classical image processing methods for fingerprint denoising propose to exploit contextual information in a fingerprint image either using ridge orientation or ridge continuity. These approaches typically employ *filtering* in spatial or frequency domain to predict ridge details in unclear or noisy regions of a fingerprint image [18, 62, 15, 7, 53]. Other approaches include using transformation such as wavelet decomposition [20] and discrete cosine transform [21]. Li *et al.* [36] propose denoising of noisy fingerprint regions using nonlocal Cahn–Hilliard equation. Gupta *et al.* [16] approximate fingerprint ridge orientation and minutiae density using higher order polynomial. Availability of reliable contextual information is a key factor to obtain satisfactory performance using these approaches. However, the extracted contextual information is often incorrect for highly noisy fingerprints. As a result, these approaches often do not generalize for heavily corrupted fingerprint regions observed in challenging real-world fingerprint samples.

2.1.2 Denoising using Learning based Methods

One of the earliest learning based approaches for fingerprint denoising include *dictionary based methods* [10, 66, 6, 37, 5, 54]. These approaches generally create a dictionary of orientation fields of fingerprint ridges. Later, the constructed dictionary is exploited to approximate fingerprint ridge orientation in fingerprint regions. However, a key limitation of these approaches arises from the fact that the dictionary of fingerprint ridge orientation is created by computing fingerprint ridge orientations on good quality fingerprint regions. As a result, these orientation approximation methods do not generally work well on heavily distorted fingerprints. To address the limitations of dictionary based fingerprint denoising methods, *orientation field prediction models* are introduced [2, 46]. These models are trained to predict the orientation field for an input patch of a fingerprint image. However, in these approaches, although the orientation fields are learnt through an orientation field prediction model, however, Gabor filtering using the predicted orientations is applied to denoise input fingerprints.

Recent research direction for fingerprint denoising exploits learnable models that *directly output the denoised fingerprint image* [48, 51, 47, 55, 45] rather than predicting the orientations of fingerprint ridges and applying contextual filtering using a Gabor filter tuned at the predicted orientations. One of the early approaches in this direction includes the contributions of Schuch *et al.* [51]. The authors propose an autoencoder architecture (DeConvNet) for fingerprint denoising. Similar to [51], Svoboda *et al.* [55] also propose an autoencoder model for fingerprint denoising. However,

Algorithm	Reference	Approach and Limitation
Classical Image Processing	Hong <i>et al.</i> [18]	Filtering using Gabor filters tuned on local ridge frequency and orientations. Correct contextual information cannot be extracted from noisy regions due to which the algorithm gives unsatisfactory performance in noisy regions.
	STFT [7]	Filtering in Fourier domain. Correct frequency information cannot be extracted from noisy regions due to which the algorithm gives unsatisfactory performance in noisy regions.
Deep learning based approaches	DeConvNet [51]	Exploits an auto-encoder network. Generates blurred fingerprints with poor ridge-valley clarity. Suffers from domain shift between training and test datasets.
	FP-E-GAN [24]	A paired image-to-image translation based generative adversarial network. Suffers from domain shift between training and test datasets.
	Svoboda <i>et al.</i> [55]	An auto-encoder based fingerprint denoising network that generates spurious ridge patterns in noisy regions. Suffers from domain shift between training and test datasets.
	Cycle-GAN [33]	An unpaired image-to-image translation based generative adversarial network. Fails to preserve ridge details in noisy regions. Suffers from domain shift between training and test datasets.
	DU-GAN [30]	Data uncertainty guided generative adversarial network for fingerprint denoising. Does not generalize on challenging latent fingerprints. Suffers from domain shift between training and test datasets.
	MU-GAN[27]	Explainable fingerprint denoising model that provides model uncertainty information. Does not generalize on challenging latent fingerprints. Suffers from domain shift between training and test datasets.
	DA-GAN (Proposed)	A paired image-to-image translation based generative model for fingerprint denoising. The model exploits auxiliary tasks to address the <i>domain shift</i> between training and test datasets.

Table 1 A table listing all the fingerprint denoising models investigated and contrasted with the proposed DA-GAN.

the proposed autoencoder minimizes orientation and gradient between the output denoised fingerprints and ground truth. Horapong *et al.* [19] suggest to identify artifacts in denoised fingerprint regions by utilizing a spectral autoencoder. Qian *et al.* [45] suggest a DenseUnet architecture for denoising fingerprint patches. Interested readers are referred to [52] for a comprehensive survey of fingerprint denoising methods.

Recently, GANs have emerged as state-of-the-art fingerprint denoising models. Joshi *et al.* suggest FP-E-GAN, a paired image to image translation GAN [24,23] to denoise fingerprint images. Karabulut *et al.* [33] suggest Cycle-GAN [68], an unpaired image to image translation based solution to fingerprint denoising. Recently, model uncertainty [29], data uncertainty [30] and channel level attention [32] are introduced into GANs to design generalizable fingerprint denoising models.

To summarize, we note the drawback of state-of-the-art that all the recent fingerprint denoising approaches that directly output the denoised fingerprint images are trained on synthetically distorted fingerprints. However, there is a visible *domain*

shift between the synthetically distorted and real low quality fingerprints. As a result, existing fingerprint denoising models suffer from poor generalization on challenging real-world fingerprint images [28, 26, 25]. This research proposes to overcome the domain shift by training a fingerprint denoising model to learn auxiliary tasks.

2.2 Unsupervised Domain Adaptation

To save the effort in human annotations and to promote transferable learning across domains, *unsupervised domain adaptation* is introduced. Domain adaptation can be performed through a variety of techniques explained next. The earliest approaches for unsupervised domain adaptation include minimization of domain discrepancy. These approaches minimize the domain discrepancy loss between the target and source image distributions such that the model learns domain-invariant features. Deep Domain Confusion [59], deep adaptation network [39] and weighted domain adaptation network [65] are some popular unsupervised domain adaptation approaches in this category.

Some prominent studies in unsupervised domain adaptation propose to adapt the domains using a reconstruction based approach. These approaches utilize a secondary reconstruction task such that the shared representation across source and target domains can be learnt [12, 17, 50, 41, 1, 8, 38]. Another important direction of research in unsupervised domain adaptation advocates to utilize an adversarial discriminator. Recently, Joshi *et al.* [31] propose an adversarial learning based domain adaptation for learning sensor-invariant features for fingerprint segmentation. Adversarial learning based domain adaptation methods employ a discriminator network to discriminate between features of source and target domain. This encourages the model to learn domain invariant features [58, 57, 40, 34, 67, 61]. For a comprehensive survey on unsupervised domain adaptation, the interested readers may refer [63].

2.3 Learning with Pseudo-Annotations

Image recognition applications where no or only limited annotations are available, pseudo-annotations can be generated for the unannotated data. Several studies demonstrate that learning with pseudo annotations facilitates improved representation learning. Towards this, Doersch *et al.* [9] propose to learn context by extracting two patches and predicting the position of the second patch with respect to the first patch. Gidaris *et al.* [14] propose to rotate image at different angles and generate pseudo annotations. Pathak *et al.* [43] propose an image painting based approach to learn context in an image. Ghifary *et al.* [13] propose a denoising based approach to facilitate improved representation learning. Motivated by the usefulness of pseudo-annotations for improved representation learning, this paper exploits pseudo-annotations to train the fingerprint denoising model to learn two auxiliary tasks, namely rotation and patch location prediction.

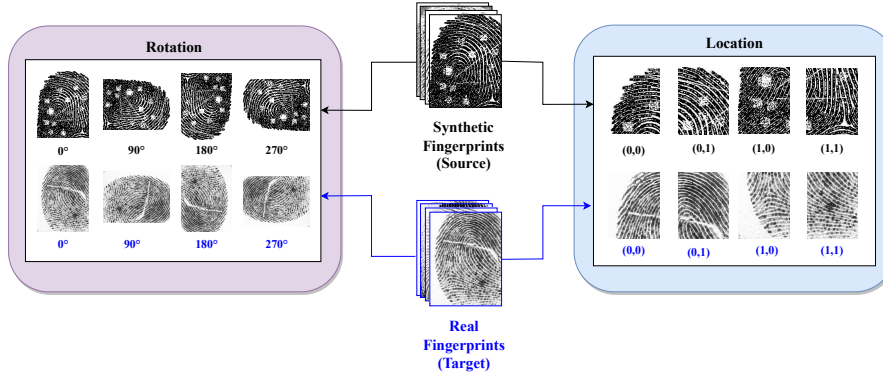


Fig. 2 Pseudo-annotations are generated for both source and target datasets for training the auxiliary tasks. To generate pseudo-annotated data for training the rotation prediction network, input fingerprint image is rotated at different angles. Likewise, to generate pseudo-annotated data for training the patch location prediction network, random patches are cropped from the input fingerprint image.

3 Proposed Method

3.1 Problem Formulation

Let X_{src} denotes the distribution of synthetically distorted fingerprints and the corresponding pixel-level annotated denoised binarized fingerprints. X_{tgt} denotes the distributions of unannotated real fingerprints. $X_{src} = \{(x_{src}, y_{src})\}$ and $X_{tgt} = \{x_{tgt}\}$. The objective is to learn a fingerprint model that achieves improved fingerprint denoising performance on real fingerprints (X_{tgt}) by aligning features of synthetic (X_{src}) and real (X_{tgt}) fingerprints.

3.2 Overview

We formulate fingerprint denoising as a multi-tasking learning based unsupervised alignment problem such that the fingerprint denoising model is trained to not only minimize the fingerprint denoising loss but two more additional losses corresponding to the two tasks auxiliary tasks, namely rotation and patch location prediction. The joint training of the fingerprint denoising task with two auxiliary tasks common to both the synthetically distorted (source) and real fingerprints (target) enforces domain alignment on the features learnt by a backbone fingerprint denoising model. This, in turn, facilitates better generalization on real noisy fingerprints.

3.3 Data Preparation for Learning Auxiliary Tasks

The auxiliary tasks are introduced to align the domains of synthetically distorted and real low quality fingerprints. However, as the annotations of real fingerprints are unavailable, the learning of auxiliary tasks is conducted using *pseudo-annotations* (see

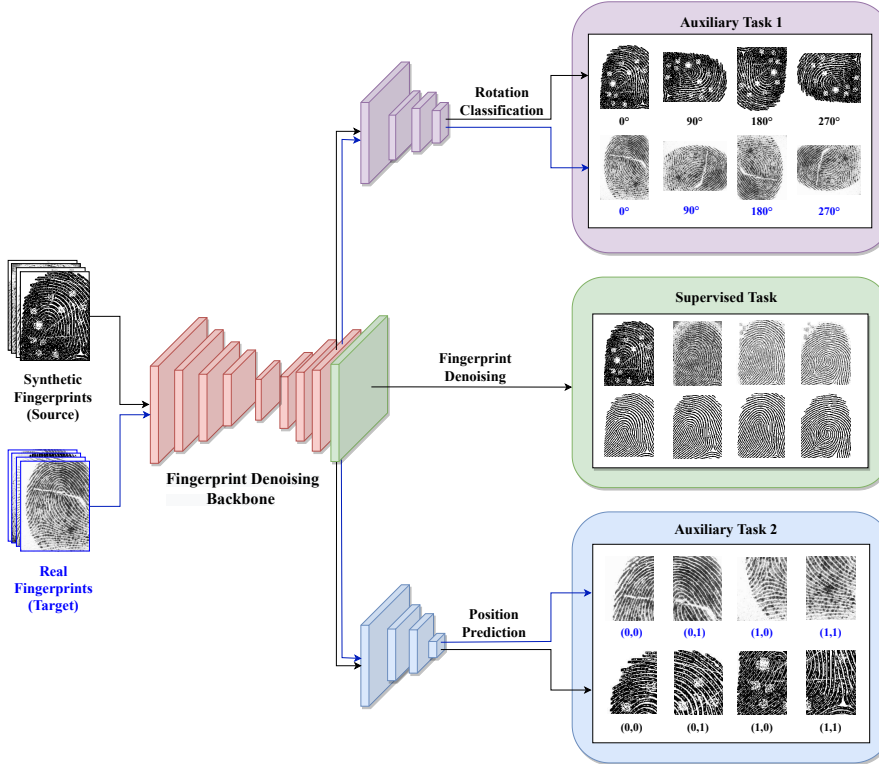


Fig. 3 Flowchart depicting proposed domain alignment using two auxiliary tasks. A multi-task learning mechanism is exploited such that fingerprint denoising is learnt using a synthetic annotated training set (source). Additionally, the model also learns to predict rotation and location on unlabelled real (target) and synthetic (source) fingerprints using pseudo-annotations. As a common fingerprint denoising backbone model is used for auxiliary tasks on both the domains, the model learns to align features of synthetic and real fingerprints.

Figure 2). For learning the *rotation prediction task*, the input fingerprint samples are rotated in increments of 90°, i.e. {0°, 90°, 180°, 270°}. Let the transformed source dataset for learning to predict rotation is represented by $T_{rot}(X_{src}) = \{(t_{rot}(x_{src}), y_{rot})\}$. Similarly, the transformed target dataset for learning to predict rotation is represented by $T_{rot}(X_{tgt}) = \{(t_{rot}(x_{tgt}), y_{rot})\}$.

Next, for learning the *patch location prediction task*, random patches are cropped from the input fingerprint image. The location prediction task is defined to predict the quadrant from which the patch is cropped. It is a two-dimensional regression problem in with pseudo-annotations defined as {(0,0), (1,0), (0,1), (1,1)}. Let the transformed source dataset for learning to predict patch location is represented by $T_{loc}(X_{src}) = \{(t_{loc}(x_{src}), y_{loc})\}$. Similarly, the transformed target dataset for learning to predict rotation is represented by $T_{loc}(X_{tgt}) = \{(t_{loc}(x_{tgt}), y_{loc})\}$.

Notation	Description
X_{src}	Source data distribution
X_{tgt}	Target data distribution
T_{rot}	Distribution of rotation transformation
y_{rot}	Ground truth rotation label
T_{loc}	Distribution of location transformation (patch extraction)
y_{loc}	Ground truth location label
t_{rot}	A given rotation transformation
t_{loc}	A given location transformation
(x_{src}, y_{src})	An annotated sample from the source dataset
x_{tgt}	An unannotated sample from the target dataset
(x_{rot}, y_{rot})	Input x rotated at angle y_{rot}
(x_{loc}, y_{loc})	Image patch extracted from input x from pixel location y_{loc}
θ	Model parameters till the penultimate layer
α	Model parameters of the last layer of the backbone model
β	Model parameter of the rotation prediction branch
γ	Model parameter of the location prediction branch
$\psi(\theta(x); \alpha)$	Denoised fingerprint output for an input x
$\psi(\theta(x); \beta)$	Predicted rotation for an input x
$\psi(\theta(x); \gamma)$	Predicted location for an input x
γ	Model parameter of the location prediction branch
\mathcal{L}_{bs}	Baseline fingerprint denoising loss
\mathcal{L}_{rot}	Rotation prediction loss
\mathcal{L}_{loc}	Location prediction loss

Table 2 Table summarizing the mathematical symbols used in the paper.

3.4 Multi-Task Fingerprint Denoising using Auxiliary Tasks

To align domains of synthetic and real fingerprints, the backbone fingerprint denoising model is modified as a multi-task learning model (see Figure 3). Let the model parameters of the backbone fingerprint denoising model be represented by $\{\theta, \alpha\}$, where θ represents the model parameters till the penultimate layer and α denotes the parameters of the last layer. Model parameters of the rotation and patch location prediction networks are represented by β and γ , respectively. For an input fingerprint x , the corresponding denoised fingerprint, predicted rotation and location are represented by $\psi(\theta(x); \alpha)$, $\psi(\theta(x); \beta)$ and $\psi(\theta(x); \gamma)$ respectively. Let L_{bs} represents the denoising loss of the baseline fingerprint denoising model. Fingerprint denoising task is learnt using only the *source* dataset by minimizing \mathcal{L}_{bs} .

$$\mathcal{L}_{bs}(X_{src}; \theta, \alpha) = \sum_{(x_{src}, y_{src}) \in X_{src}} L_{bs}(\psi(\theta(x_{src}); \alpha), y_{src}) \quad (1)$$

Let L_{rot} represents the cross-entropy loss function used to train the auxiliary rotation task. Rotation task is learnt using the *transformed source and target* dataset by minimizing \mathcal{L}_{rot} .

$$\begin{aligned} \mathcal{L}_{rot}(X_{src}, X_{trgt}; \theta, \beta) = & \sum_{(x_{rot}, y_{rot}) \in T_{rot}(X_{src})} L_{rot}(\psi(\theta(x_{rot}); \beta), y_{rot}) + \\ & \sum_{(x_{rot}, y_{rot}) \in T_{rot}(X_{tgt})} L_{rot}(\psi(\theta(x_{rot}); \beta), y_{rot}) \end{aligned} \quad (2)$$

Similarly, Let L_{loc} represents the regression based loss function used to train the auxiliary patch location prediction task. Location prediction task is learnt using the *transformed source and target* dataset by minimizing \mathcal{L}_{loc} .

$$\begin{aligned} \mathcal{L}_{loc}(X_{src}, X_{trgt}; \theta, \gamma) = & \sum_{(x_{loc}, y_{loc}) \in T_{loc}(X_{src})} L_{loc}(\psi(\theta(x_{loc}); \gamma), y_{loc}) + \\ & \sum_{(x_{loc}, y_{loc}) \in T_{loc}(X_{tgt})} L_{loc}(\psi(\theta(x_{loc}); \gamma), y_{loc}) \end{aligned} \quad (3)$$

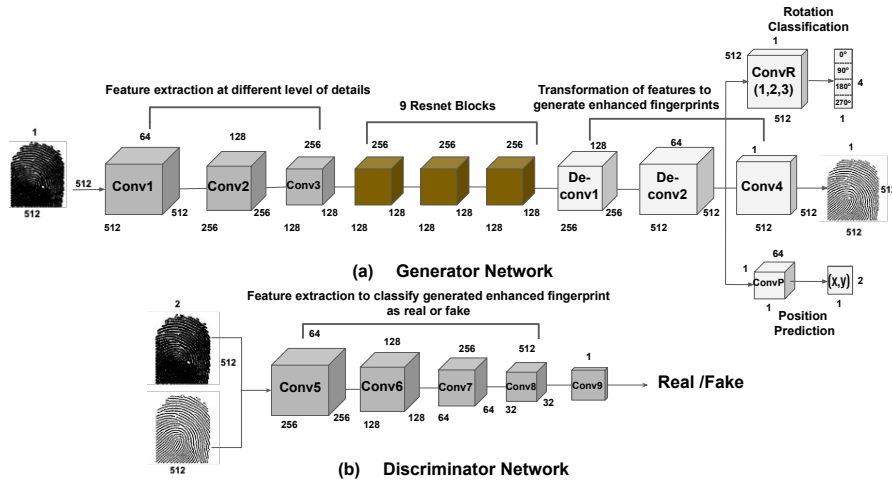
Note that the baseline fingerprint denoising task is trained using $\mathcal{L}_{bs}(X_{src}; \theta, \alpha)$ and takes only the *annotated source dataset* as the input. On the other hand, both the auxiliary tasks of rotation and location prediction trained using $\mathcal{L}_{rot}(X_{src}, X_{trgt}; \theta, \beta)$ and $\mathcal{L}_{loc}(X_{src}, X_{trgt}; \theta, \gamma)$ respectively take pseudo-annotated data corresponding to *both the source and target domains* as the input. Joint training of the three loss functions enforces domain alignment. The total loss minimized by the fingerprint denoising model is formalized as:

$$\arg \min_{(\theta, \alpha, \beta, \gamma)} [\mathcal{L}_{bs}(X_{src}; \theta, \alpha) + \mathcal{L}_{rot}(X_{src}, X_{trgt}; \theta, \beta) + \mathcal{L}_{loc}(X_{src}, X_{trgt}; \theta, \gamma)] \quad (4)$$

For an input fingerprint x , for inference during test-time, the sub-networks pertaining to the auxiliary tasks are discarded, and only the output of the fingerprint denoising task, i.e., $\psi(\theta(x); \alpha)$ is used. In this paper, as suggested in Section 3, we modify the backbone fingerprint denoising model, FP-E-GAN [24] and propose DA-GAN (Domain Aligned GAN).

4 Implementation Details

We proceed to elaborate the network design of DA-GAN. Figure 4 illustrates different convolution blocks constituting the fingerprint denoising model as well as branches for auxiliary tasks, rotation and location prediction. Details on the convolution layer characteristics and activation functions is provided in Table 3 and Table 4. The synthetic noisy and corresponding good quality fingerprints are obtained as per guidelines provided in [23, 24]. The source code of DA-GAN is implemented in PyTorch, v1.11.0. Adam optimizer with a learning rate of 0.0002 is used to optimize the loss function of DA-GAN. Training of DA-GAN is conducted on four NVIDIA GTX 1080 Ti GPUs and a E5-2620v4 CPU. Each GPU has a 11 GB RAM.

**Fig. 4** Network architecture of DA-GAN.

Block	Kernels	Size	Stride	Padding	Layers
Conv1	64	7	1	3	Conv. Layer + Batch Norm + ReLu
Conv2	128	3	2	1	Conv. Layer + Batch Norm + ReLu + Conv. Layer + Batch Norm
Conv3	256	3	2	1	Conv. Layer + Batch Norm + ReLu + Conv. Layer + Batch Norm
ResNet Block	256	3	2	1	Conv. Layer + Batch Norm + ReLu + Conv. Layer + Batch Norm
Deconv1	128	3	2	1	Conv. Layer + Batch Norm + ReLu + Conv. Layer + Batch Norm
Deconv2	64	3	2	1	Conv. Layer + Batch Norm + ReLu + Conv. Layer + Batch Norm
Conv4	1	7	1	3	Conv. Layer + Tanh
ConvR-1	64	3	1	1	Conv. Layer + Batch Norm + ReLu
ConvR-2	128	3	1	1	Conv. Layer + Batch Norm + ReLu
ConvR-3	64	1	1	0	Conv. Layer + Batch Norm + ReLu
ConvP	64	1	1	0	Adaptive Pooling + Conv. Layer

Table 3 Network architecture of the generator module of DA-GAN.

Block	Kernels	Size	Stride	Padding	Layers
Conv5	64	4	2	1	Conv. Layer + LeakyReLu
Conv6	128	4	2	1	Conv. Layer + Batch Norm + LeakyReLu
Conv7	256	4	2	1	Conv. Layer + Batch Norm + LeakyReLu
Conv8	512	4	1	1	Conv. Layer + Batch Norm + LeakyReLu
Conv9	1	4	1	1	Conv. Layer

Table 4 Network architecture of the discriminator module of DA-GAN.

5 Experimental Evaluation

5.1 Databases

Noise in fingerprint images typically originates from structured noise in the background or poor skin quality of fingertips. To assess the fingerprint denoising performance under complex background, the fingerprint denoising performance on latent fingerprints is studied. Furthermore, to study the fingerprint denoising performance under poor skin quality co-variates, the proposed fingerprint denoising model is evaluated on two poor quality fingerprints databases obtained from rural Indian subjects. Next, we share details on these databases.

1. *IIITD-MOLF* [49]: IIITD-MOLF is the largest latent fingerprint database in the public domain with 4400 latent fingerprint images. Latent fingerprints in the dataset are used as the probe set, while the fingerprints acquired through the multi-spectral sensor is used as the gallery set.
2. *Rural Indian Fingerprint database* [44]: This database contains fingerprint samples of the rural Indian population involved in excessive manual work. The volunteers for database collection comprise farmers, carpenters, and villagers. This database constitutes ten impressions per finger with a total of 1631 fingerprint images.
3. A private rural fingerprint database acquired from elderly rural Indian population and population with severely poor fingertip quality. This database constitutes two impressions per finger with a total of 1000 fingerprint images.

5.2 Evaluation Metrics

1. *Fingerprint Quality Scores*: A fingerprint denoising model is introduced in a automated fingerprint recognition pipeline to improve the clarity of ridges and valleys. Therefore, one of the evaluation metrics we use in this study is to evaluate the fingerprint quality of the denoised fingerprint image. The fingerprint quality score is obtained using NBIS [42], an open source tool provided by the national institute of standards and technology (NIST).
2. *Fingerprint Matching Performance*: A fingerprint denoising model is required to generate fingerprint images that obtain higher match scores on genuine matches, thus better matching performance. Towards evaluating the improvement in matching performance, we compare cumulative matching characteristics (CMC) curves for latent fingerprints and average equal error rate (EER) for both the rural Indian fingerprint databases. Standard fingerprint matching tools, Bozorth [42] and MCC [4], [3] and [11] are used to perform fingerprint matching.

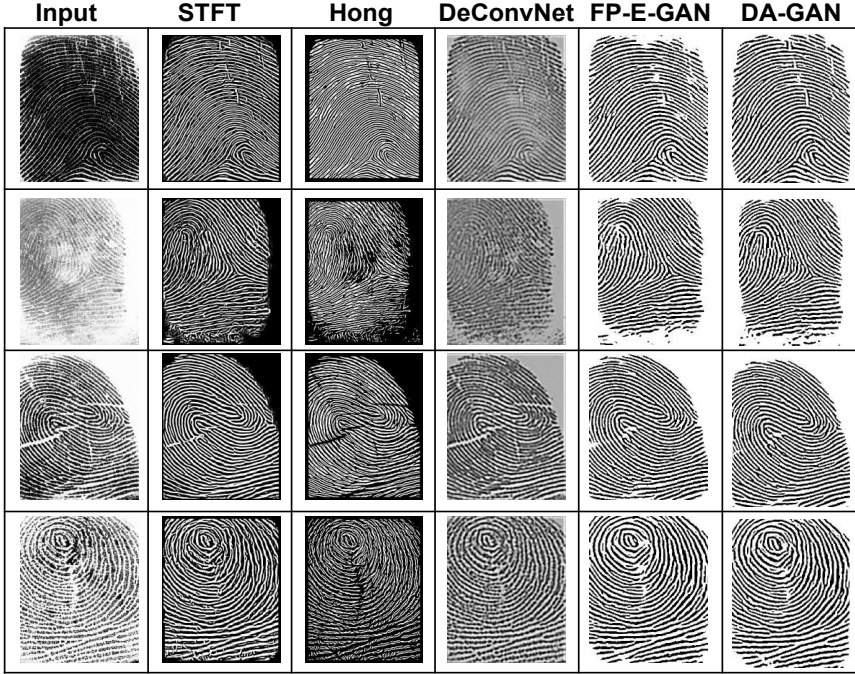


Fig. 5 Existing fingerprint denoising models perform worse than DA-GAN in predicting unclear and missing ridge details due to dry and wet fingertips or creases and scars.

Denoising Algorithm	Algo-	Avg. Quality Score (\downarrow)
Raw Image		2.94
STFT [7]		2.86
Hong <i>et al.</i> [18]		2.05
DeconvNet [51]		1.95
FP-E-GAN [24]		1.31
DA-GAN		1.28

Table 5 Average fingerprint quality scores obtained on the rural Indian fingerprint database [44]. The results indicate that improved quality denoised fingerprints are obtained after introducing the proposed domain alignment framework.

Denoising Algorithm	Algo-	Bozorth (\downarrow)	MCC (\downarrow)
Raw Image		16.36	13.23
STFT [7]		18.13	14.52
Hong <i>et al.</i> [18]		11.01	11.46
DeConvNet [51]		10.93	10.86
FP-E-GAN [24]		7.30	5.96
DA-GAN		6.10	5.31

Table 6 Average EER obtained on the rural Indian fingerprint database [44] using Bozorth and MCC matchers. The results indicate that improved fingerprint matching performance is obtained after introducing the proposed domain alignment framework.

6 Comparison with State-of-the-art

6.1 Performance on Rural Indian Fingerprints

Figure 5 contrasts state-of-the-art fingerprint denoising algorithms with DA-GAN. These results demonstrate that the proposed DA-GAN is able to predict unclear and missing ridge details due to dry and wet fingertips or creases and scars. Thus, fa-

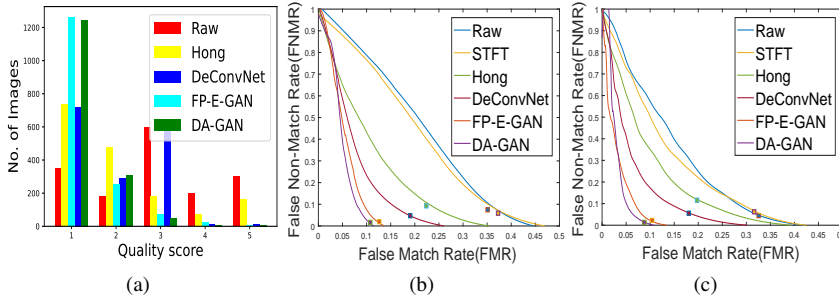


Fig. 6 (a) Histogram of fingerprint quality scores and DET curves for (b) Bozorth (c) MCC. On the rural Indian fingerprint database [44], DA-GAN greatly outperforms contemporary fingerprint denoising techniques.

Denoising algorithm	Algo-	Avg. Quality Score (\downarrow)
DeConvNet [51]		4.12
FP-E-GAN [24]		2.28
DA-GAN		1.94

Table 7 Average fingerprint quality scores obtained on the private rural fingerprint database.

Denoising algorithm	Algo-	Bozorth (\downarrow)	MCC (\downarrow)
DeConvNet [51]		28.75	26.80
FP-E-GAN [24]		17.06	15.85
DA-GAN		11.53	9.70

Table 8 Average EER obtained on the private rural Indian fingerprint database.

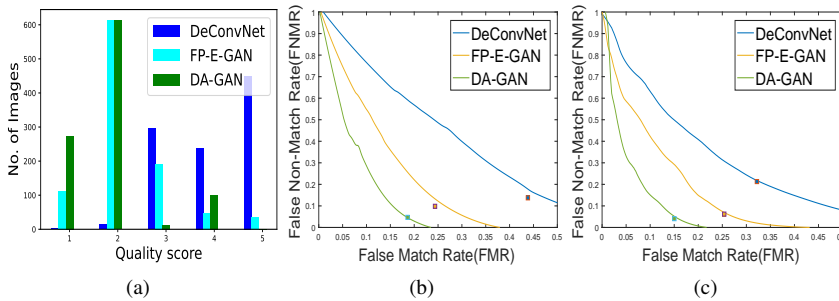


Fig. 7 (a) Histogram of fingerprint quality scores and DET curves for (b) Bozorth (c) MCC. On the private rural Indian fingerprint database, DA-GAN greatly outperforms contemporary fingerprint denoising techniques.

cilitating improved fingerprint matching performance. We now present a quantitative analysis of the findings from the rural Indian fingerprint database. Table 5 reports that the average fingerprint quality scores has improved from 1.31 to 1.28 after domain alignment (lower quality scores indicates better fingerprint quality scores). These results demonstrate that the proposed domain alignment framework helps to obtain better fingerprint denoising performance on challenging rural Indian fingerprints.

Next, to quantify the improvement in matching performance, Table 6 reports that the average EER has improved from 7.30 to 6.10 for Bozorth matcher and 5.96 to 5.31 for MCC matcher. Corresponding histogram of fingerprint quality scores and

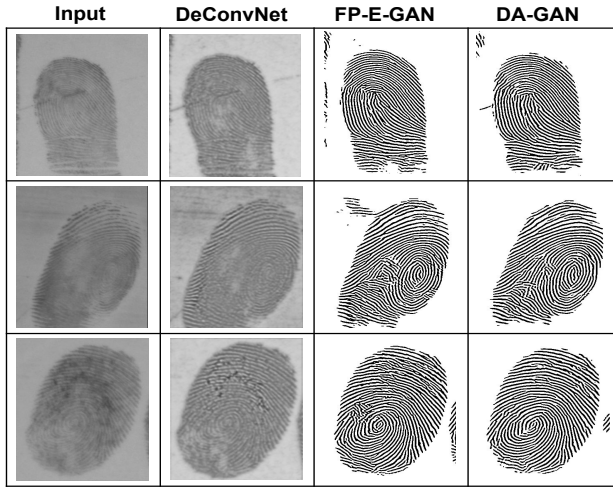


Fig. 8 Sample cases demonstrating improved fingerprint denoising ability of DA-GAN in contrast to state-of-the-art on the IIITD-MOLF database.

Denoising Algorithm	Algo-	Avg. Quality Score (\downarrow)
Raw Image		4.96
DeConvNet [51]		4.09
FP-E-GAN [24]		1.91
DA-GAN		2.03

Table 9 Average fingerprint quality scores obtained on the IIITD-MOLF database.

Denoising Algorithm	Algo-	Bozorth (\uparrow)	MCC (\uparrow)
Raw Image		5.45	6.06
DeConvNet [51]		14.02	14.27
Svoboda <i>et al.</i> [55]		NA	22.36
FP-E-GAN [24]		28.52	34.43
DA-GAN		29.61	36.06

Table 10 Rank-50 accuracy obtained on the IIITD-MOLF database.

detection error tradeoff (DET) curves are plotted in Figure 6 (a) and Figure 6 (b)-(c) respectively. Similar trends are reported for the private rural Indian fingerprint database in which the average EER has improved from 17.06 to 11.53 for Bozorth matcher and 15.85 to 9.70 for MCC matcher. Corresponding results are reported in Table 7, Table 8 and Figure 7.

6.2 Performance on Latent Fingerprints

We demonstrate that the domain alignment of fingerprint denoising models generalizes on latent fingerprints. Sample denoised fingerprints obtained by the proposed DA-GAN are compared to the state-of-the-art in Figure 8. DA-GAN generates fewer spurious ridge patterns in the background and unclear fingerprint image regions compared to the state-of-the-art. Next, we quantify the improvement in fingerprint denoising performance. We find that the rank-50 identification accuracy improves from 28.52 to 29.60 on the Bozorth fingerprint matcher and from 34.43 to 36.06 on the MCC matcher, after proposed domain alignment. We find that the fingerprint quality

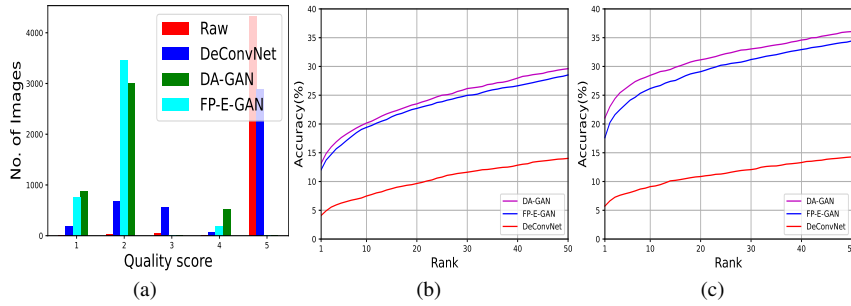


Fig. 9 Comparison of fingerprint denoising performance obtained by the proposed DA-GAN and state-of-the-art on the IIITD-MOLF database: (a) histogram of fingerprint quality scores; identification performance characterized by CMC curves using fingerprint matching tools (b) Bozorth (c) MCC.

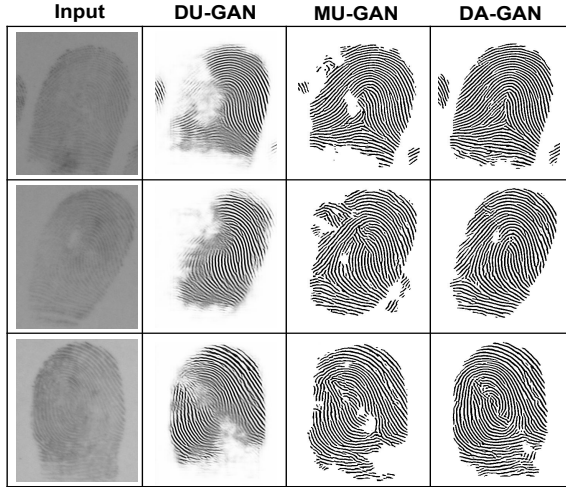


Fig. 10 Sample denoised fingerprints from the IIITD-MOLF database comparing the proposed DA-GAN with recent GAN based fingerprint denoising models.

is also competitive to the baseline. Fingerprint quality scores and rank-50 accuracy are reported in Table 9 and Table 10 respectively. Figure 9 shows the respective histograms of fingerprint quality scores and CMC curves. These results clearly establish the fact that domain alignment helps to improve the performance of a fingerprint denoising model.

6.3 Comparison with Recent GAN based Fingerprint Denoising Models

Proposed DA-GAN significantly outperforms recently proposed generative adversarial network (GAN) based state-of-the-art fingerprint denoising models. Denoised fingerprints generated by the proposed DA-GAN obtain the highest rank-50 accuracy on both the fingerprint matchers. Although MU-GAN [27] obtains better average fin-

Denoising Algorithm	Avg. Quality Score (\downarrow)
Cycle-GAN [33]	4.90
DU-GAN [30]	3.01
MU-GAN[27]	1.48
DA-GAN	2.03

Table 11 Comparison of average fingerprint quality scores obtained by the proposed DA-GAN and recent GAN based state-of-the-art fingerprint denoising models on the IIITD-MOLF database.

Denoising Algorithm	Algo- (\uparrow)	Bozorth (\uparrow)	MCC (\uparrow)
Cycle-GAN [33]	6.29	4.65	
DU-GAN [30]	23.16	27.21	
MU-GAN [27]	25.09	28.61	
DA-GAN	29.61	36.06	

Table 12 Rank-50 accuracy obtained by the proposed DA-GAN and recent GAN based state-of-the-art fingerprint denoising models on the IIITD-MOLF database.

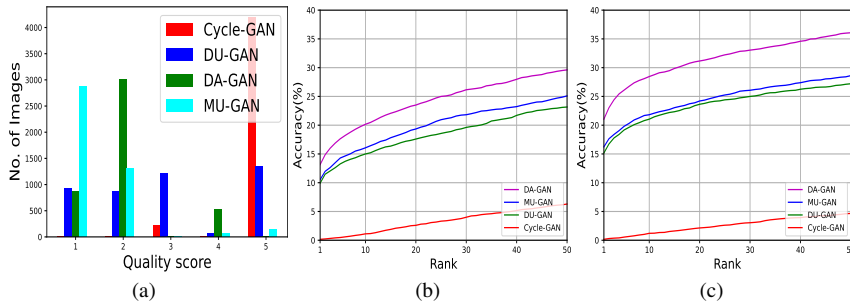


Fig. 11 Comparison of fingerprint denoising performance obtained by the proposed DA-GAN and the recent GAN based fingerprint denoising models on the IIITD-MOLF database: (a) histogram of fingerprint quality scores; identification performance characterized by CMC curves using fingerprint matching tools (b) Bozorth (c) MCC.

gerprint quality scores as compared to the proposed DA-GAN; however, this is due to the limitation of the fingerprint quality assessment tool provided by NBIS [42]. Figure 10 compares the samples generated by the proposed DA-GAN with the state-of-the-art. These samples demonstrate that MU-GAN sometimes does not reconstruct the fingerprint ridge details on poor quality fingerprint regions, as opposed to the proposed DA-GAN. Poor ridge smoothness on such reconstructed ridges attributes to the second-best fingerprint quality scores obtained by the proposed DA-GAN. However, since the minutiae details are preserved while denoising such poor quality fingerprint regions, the proposed DA-GAN achieves the highest rank-50 accuracy (see Table 11, Table 12 and Figure 11).

6.4 Comparison of Computational Complexity

We begin the comparison of computational complexity of the proposed DA-GAN with state-of-the-art (hyperparameters reported in Table 13) by comparing the model capacity characterized by number of model parameters. As reported in Table 14, Cycle-GAN has the highest number of model parameters which makes it prone to overfitting and poor generalization. MU-GAN has the least number of parameters,

Denoising Algorithm	Learning Rate	Batch Size
Cycle-GAN [33]	0.0002	1
DU-GAN [30]	0.0002	2
MU-GAN [27]	0.0002	2
DA-GAN	0.0002	1

Table 13 Hyperparameters for the proposed DA-GAN and recent GAN based state-of-the-art fingerprint denoising models.

Denoising Algorithm	Model Parameters (in millions)
Cycle-GAN [33]	114.32
DU-GAN [30]	14.16
MU-GAN [27]	14.14
DA-GAN	15.33

Table 14 Comparison of model parameters of the proposed DA-GAN and recent GAN based state-of-the-art fingerprint denoising models.

Denoising Algorithm	GFLOPS
Cycle-GAN [33]	168.26
DU-GAN [30]	237.54
MU-GAN [27]	238.28
DA-GAN	277.12

Table 15 Comparison of GFLOPS required by the proposed DA-GAN and recent GAN based state-of-the-art fingerprint denoising models.

however the models parameters of the proposed DA-GAN is competitive to MU-GAN with far better denoising ability, which confirms the superiority of the proposed DA-GAN.

Next, we compare the computational head of the proposed DA-GAN with state-of-the-art by comparing the number of GFLOPS. As reported in Table 15, Cycle-GAN has the lowest computational overhead, however the least denoising capability. DA-GAN has the highest computational complexity. However, the computational overhead of DA-GAN is competitive to DU-GAN and MU-GAN while providing the best denoising performance. These results demonstrate the efficacy of the proposed DA-GAN over state-of-the-art.

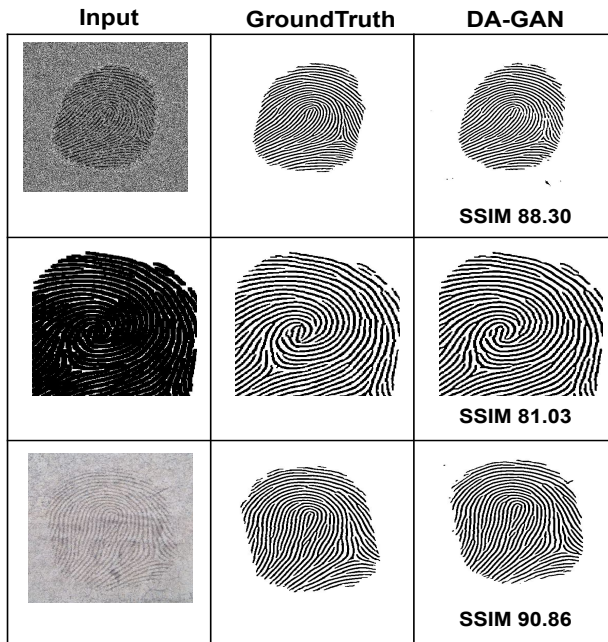


Fig. 12 Sample synthetic test cases illustrating the ridge preservation ability of DA-GAN.

7 Model Analysis

7.1 Ridge Preservation Ability

A low quality fingerprint image is characterized by the presence of structured noise in the background or blurred ridges. A fingerprint denoising model is required to eliminate noise while preserving ridge details. Figure 12 demonstrates that a high structural similarity index metric (SSIM) between the denoised fingerprint and the ground truth is obtained for DA-GAN. These results demonstrate that the proposed DA-GAN preserves ridge details of fingerprints including ridge orientation and minutiae while denoising them.

Auxiliary Task	Avg. Quality Score (.)
Baseline	1.31
Rotation	1.34
Location	1.37
Both	1.28

Table 16 Average fingerprint quality scores obtained on the rural Indian fingerprint database for the ablation study.

Auxiliary Task	Bozorth (.)	MCC (.)
Baseline	7.30	5.96
Rotation	6.67	5.82
Location	6.73	5.70
Both	6.10	5.31

Table 17 Average EER obtained on the rural Indian fingerprint database for the ablation study.

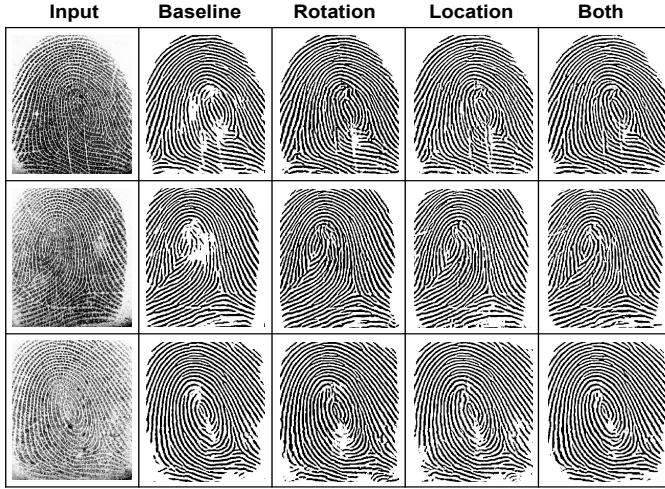


Fig. 13 Sample cases comparing the impact of each auxiliary task.

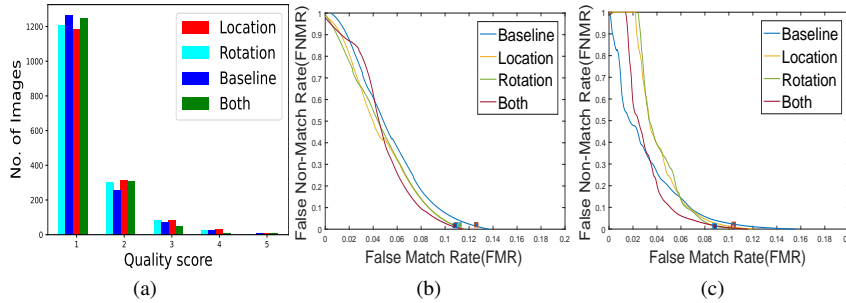


Fig. 14 (a) Histogram of fingerprint quality scores and DET curves for (b) Bozorth (c) MCC. Fingerprint denoising performance is improved on the rural Indian fingerprint database [44] after introducing each auxiliary task: location and rotation prediction. As expected, best fingerprint denoising performance is obtained after introduction of both the auxiliary tasks.

7.2 Significance of Each Auxiliary Task

Next, we investigate the individual contribution of each auxiliary task in facilitating domain alignment and, subsequently, improved fingerprint denoising performance. Samples presented in Figure 13 demonstrate that the fingerprint denoising performance of the baseline (FP-E-GAN) fingerprint denoising model improves by introducing either of the auxiliary task, location, or rotation prediction. Location prediction turns out to be more significant compared to rotation prediction. However, the introduction of both the auxiliary tasks renders the best fingerprint denoising performance. Improved fingerprint quality scores and matching performance are obtained after the introduction of the auxiliary tasks, as reported in Table 16 and Table 17. The corresponding histogram of fingerprint quality scores and DET curves are plotted in Figure 14.



Fig. 15 Sample successful fingerprint denoising cases for the proposed DA-GAN.

7.3 Successful Cases

Figure 15 demonstrates successful sample cases of fingerprint denoising by DA-GAN. We observe that DA-GAN successfully predicts missing ridge details due to creases or smudged ridge patterns. Similarly, for fingerprint samples with unclear valley details due to thick ridges or samples with non-uniform chemical powder, the proposed DA-GAN successfully executes fingerprint denoising. These outcomes illustrate the generalization of DA-GAN on challenging latent and rural Indian fingerprints.

7.4 Challenging Cases

Figure 16 contrasts the denoised fingerprints output by DA-GAN with the ones obtained using existing fingerprint denoising models on challenging samples. The first row depicts that the proposed DA-GAN predicts spurious ridge patterns around the scarred fingerprint region. The second row depicts dark ridges in fingerprint regions with high pressure. Around high-pressure regions, DU-GAN predicts non-smooth and spurious ridges. However, in all the presented cases, denoising ability of DA-GAN is superior to state-of-the-art and the baseline FP-E-GAN. These results confirm that the proposed unsupervised domain alignment improves fingerprint denoising performance.

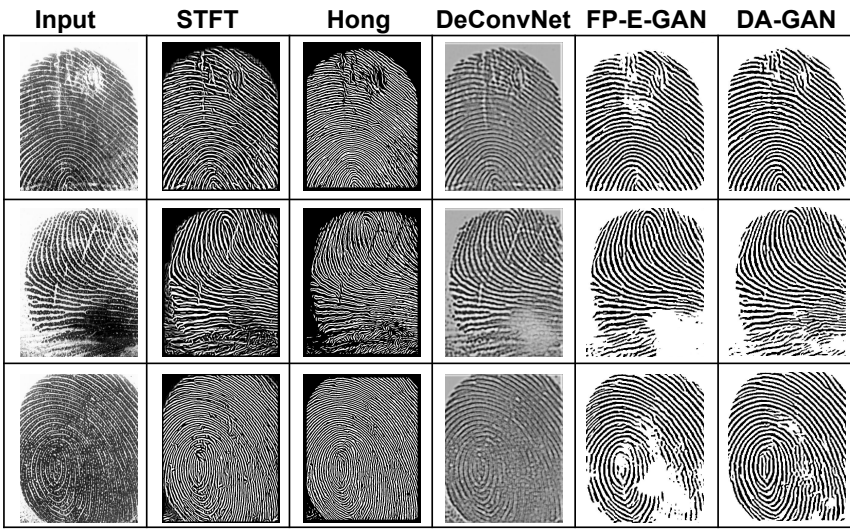


Fig. 16 Comparison of the proposed DA-GAN with state-of-the-art fingerprint denoising models on challenging samples.

8 Conclusion

This research highlights the limitation in the generalization ability of state-of-the-art fingerprint denoising models due to training on synthetic data. To counter the domain shift that exists between synthetically distorted and real low quality fingerprints, this research proposes multi-task learning using two auxiliary tasks, rotation and location prediction. Results reveal that the proposed unsupervised domain alignment improves the performance of a fingerprint denoising model. However, we find that there is further scope to improve denoising performance in significantly noisy fingerprint regions (discussed in Section 7.4) by exploiting contextual information. In future, the proposed domain alignment technique can be exploited to reduce the domain gap observed during other stages of an automated fingerprint recognition system, such as region of interest segmentation and presentation attack detection.

9 Acknowledgement

The authors acknowledge the support of the HPC services of Inria Sophia Antipolis and IIT Delhi for the computational infrastructure. The authors sincerely thank Prof. Phalguni Gupta from IIT Kanpur and Prof. Kamlesh Tiwari from BITS Pilani for sharing the private rural Indian fingerprint used in this research. The authors acknowledge Naman Mukund from Tekie for his technical guidance.

10 Declarations

This work is partly supported by the French government, the National Research Agency (ANR) under grant ANR-18-CE92-0024, project RESPECT.

11 Competing Interests

A. Dantcheva, one of the co-authors of this manuscript is a member of the editorial board of this journal.

12 Data Availability Statement

Data sharing not applicable to this article as no datasets were generated or analyzed during the current study.

References

1. Bousmalis, K., Silberman, N., Dohan, D., Erhan, D., Krishnan, D.: Unsupervised Pixel-Level Domain Adaptation with Generative Adversarial Networks. In: Proc. IEEE International Conference on Computer Vision and Pattern Recognition (CVPR), pp. 3722 – 3731 (2017)
2. Cao, K., Jain, A.K.: Latent Orientation Field Estimation via Convolutional Neural Network. In: Proc. International Conference on Biometrics (ICB), pp. 349 – 356 (2015)
3. Cappelli, R., Ferrara, M., Maltoni, D.: Fingerprint Indexing Based on Minutia Cylinder-Code. *IEEE Transactions on Pattern Analysis and Machine Intelligence* **33**(5), 1051 – 1057 (2010)
4. Cappelli, R., Ferrara, M., Maltoni, D.: Minutia Cylinder-Code: A New Representation and Matching Technique for Fingerprint Recognition. *IEEE Transactions on Pattern Analysis and Machine Intelligence* **32**(12), 2128 – 2141 (2010)
5. Chaidee, W., Horapong, K., Areekul, V.: Filter Design Based on Spectral Dictionary for Latent Fingerprint Pre-Enhancement. In: Proc. International Conference on Biometrics (ICB), pp. 23 – 30 (2018)
6. Chen, C., Feng, J., Zhou, J.: Multi-Scale Dictionaries Based Fingerprint Orientation Field Estimation. In: Proc. International Conference on Biometrics (ICB), pp. 1 – 8 (2016)
7. Chikkerur, S., Cartwright, A.N., Govindaraju, V.: Fingerprint Enhancement using STFT Analysis. *Pattern Recognition* **40**(1), 198 – 211 (2007)
8. Choi, Y., Choi, M., Kim, M., Ha, J.W., Kim, S., Choo, J.: Stargan: Unified Generative Adversarial Networks for Multi-Domain Image-to-Image Translation. In: Proceedings of the IEEE conference on computer vision and pattern recognition, pp. 8789 – 8797 (2018)
9. Doersch, C., Gupta, A., Efros, A.A.: Unsupervised Visual Representation Learning by Context Prediction. In: Proc. IEEE International Conference on Computer Vision and Pattern Recognition (CVPR), pp. 1422 – 1430 (2015)
10. Feng, J., Zhou, J., Jain, A.K.: Orientation Field Estimation for Latent Fingerprint Enhancement. *IEEE Transactions on Pattern Analysis and Machine Intelligence* **35**(4), 925 – 940 (2013)
11. Ferrara, M., Maltoni, D., Cappelli, R.: Noninvertible Minutia Cylinder-Code Representation. *IEEE Transactions on Information Forensics and Security* **7**(6), 1727 – 1737 (2012)
12. Ghifary, M., Kleijn, W.B., Zhang, M., Balduzzi, D.: Domain Generalization for Object Recognition with Multi-Task Autoencoders. In: Proc. IEEE International Conference on Computer Vision (ICCV), pp. 2551 – 2559 (2015)
13. Ghifary, M., Kleijn, W.B., Zhang, M., Balduzzi, D., Li, W.: Deep Reconstruction-Classification Networks for Unsupervised Domain Adaptation. In: Proc. European conference on computer vision (ECCV), pp. 597 – 613 (2016)
14. Gidaris, S., Singh, P., Komodakis, N.: Unsupervised Representation Learning by Predicting Image Rotations. In: Proc. International Conference on Learning Representations (ICLR) (2018)

15. Gottschlich, C.: Curved-Region-Based Ridge Frequency Estimation and Curved Gabor Filters for Fingerprint Image Enhancement. *IEEE Transactions on Image Processing* **21**(4), 2220 – 2227 (2011)
16. Gupta, R., Khari, M., Gupta, D., Crespo, R.G.: Fingerprint Image Enhancement and Reconstruction using the Orientation and Phase Reconstruction. *Information Sciences* **530**, 201 – 218 (2020)
17. Hoffman, J., Tzeng, E., Park, T., Zhu, J.Y., Isola, P., Saenko, K., Efros, A., Darrell, T.: Cycada: Cycle-Consistent Adversarial Domain Adaptation. In: Proc. International Conference on Machine Learning (ICML), pp. 1989 – 1998 (2018)
18. Hong, L., Wan, Y., Jain, A.: Fingerprint Image Enhancement: Algorithm and Performance Evaluation. *IEEE Transactions on Pattern Analysis and Machine Intelligence* **20**(8), 777 – 789 (1998)
19. Horapong, K., Srisutheenon, K., Areekul, V.: Progressive and Corrective Feedback for Latent Fingerprint Enhancement using Boosted Spectral Filtering and Spectral Autoencoder. *IEEE Access* **9**, 96288 – 96308 (2021)
20. Hsieh, C.T., Lai, E., Wang, Y.C.: An Effective Algorithm for Fingerprint Image Enhancement Based on Wavelet Transform. *Pattern Recognition* **36**(2), 303 – 312 (2003)
21. Jirachaweng, S., Areekul, V.: Fingerprint Enhancement Based on Discrete Cosine Transform. In: Proc. International Conference on Biometrics (ICB), pp. 96 – 105 (2007)
22. Joshi, I.: Advanced Deep Learning Techniques for Fingerprint Preprocessing. Ph.D. thesis, IIT Delhi (2021)
23. Joshi, I., Anand, A., Dutta Roy, S., Kalra, P.K.: On Training Generative Adversarial Network for Enhancement of Latent Fingerprints. In: AI and Deep Learning in Biometric Security, pp. 51 – 79 (2021)
24. Joshi, I., Anand, A., Vatsa, M., Singh, R., Dutta Roy, S., Kalra, P.: Latent Fingerprint Enhancement using Generative Adversarial Networks. In: IEEE Winter Conference on Applications of Computer Vision (WACV), pp. 895 – 903 (2019)
25. Joshi, I., Dhamija, T., Kumar, R., Dantcheva, A., Dutta Roy, S., Kalra, P.K.: Cross-Domain Consistent Fingerprint Denoising. *IEEE Sensors Letters* (2022)
26. Joshi, I., Grimmer, M., Rathgeb, C., Busch, C., Bremond, F., Dantcheva, A.: Synthetic Data in Human Analysis: A Survey. *arXiv preprint arXiv:2208.09191* (2022)
27. Joshi, I., Kothari, R., Utkarsh, A., Kurmi, V.K., Dantcheva, A., Dutta Roy, S., Kalra, P.K.: Explainable Fingerprint ROI Segmentation using Monte Carlo Dropout. In: IEEE Winter Conference on Applications of Computer Vision Workshops (WACVW), pp. 60 – 69 (2021)
28. Joshi, I., Prakash, T., Jaiswal, B., Kumar, R., Dantcheva, A., Dutta Roy, S., Kalra, P.K.: Context-aware Restoration of Noisy Fingerprints. *IEEE Sensors Letters* (2022)
29. Joshi, I., Utkarsh, A., Kothari, R., Kurmi, V.K., Dantcheva, A., Dutta Roy, S., Kalra, P.K.: On Estimating Uncertainty of Fingerprint Enhancement Models. In: Digital Image Enhancement and Reconstruction (2022)
30. Joshi, I., Utkarsh, A., Kothari, R., Kurmi, V.K., Dantcheva, A., Dutta Roy, S., Kalra, P.K.: Data Uncertainty Guided Noise-Aware Preprocessing of Fingerprints. In: International Joint Conference on Neural Networks (IJCNN), pp. 1 – 8 (2021)
31. Joshi, I., Utkarsh, A., Kothari, R., Kurmi, V.K., Dantcheva, A., Dutta Roy, S., Kalra, P.K.: Sensor-Invariant Fingerprint ROI Segmentation using Recurrent Adversarial Learning. In: International Joint Conference on Neural Networks (IJCNN), pp. 1 – 8 (2021)
32. Joshi, I., Utkarsh, A., Singh, P., Dantcheva, A., Dutta Roy, S., Kalra, P.K.: On Restoration of Degraded Fingerprints. *Multimedia Tools and Applications* pp. 1–29 (2022)
33. Karabulut, D., Tertychnyi, P., Arslan, H.S., Ozcinar, C., Nasrollahi, K., Valls, J., Vilaseca, J., Moeslund, T.B., Anbarjafari, G.: Cycle-Consistent Generative Adversarial Neural Networks based Low Quality Fingerprint Enhancement. *Multimedia Tools and Applications* **79**(25), 18569 – 18589 (2020)
34. Li, H., Pan, S.J., Wang, S., Kot, A.C.: Domain Generalization with Adversarial Feature Learning. In: Proc. IEEE International Conference on Computer Vision and Pattern Recognition (CVPR), pp. 5400 – 5409 (2018)
35. Li, J., Feng, J., Kuo, C.C.J.: Deep Convolutional Neural Network for Latent Fingerprint Enhancement. *Signal Processing: Image Communication* **60**, 52 – 63 (2018)
36. Li, Y., Xia, Q., Lee, C., Kim, S., Kim, J.: A robust and efficient fingerprint image restoration method based on a phase-field model. *Pattern Recognition* **123**, 108405 (2022)
37. Liu, S., Liu, M., Yang, Z.: Sparse Coding Based Orientation Estimation for Latent Fingerprints. *Pattern Recognition* **67**, 164 – 176 (2017)
38. Liu, Y.C., Yeh, Y.Y., Fu, T.C., Wang, S.D., Chiu, W.C., Wang, Y.C.F.: Detach and Adapt: Learning Cross-Domain Disentangled Deep Representation. In: Proc. IEEE International Conference on Computer Vision and Pattern Recognition (CVPR), pp. 8867 – 8876 (2018)

39. Long, M., Cao, Y., Wang, J., Jordan, M.: Learning Transferable Features with Deep Adaptation Networks. In: Proc. International Conference on Machine Learning (ICML), pp. 97 – 105 (2015)
40. Long, M., Cao, Z., Wang, J., Jordan, M.I.: Conditional Adversarial Domain Adaptation pp. 1647 – 1657 (2017)
41. Murez, Z., Kolouri, S., Kriegman, D., Ramamoothi, R., Kim, K.: Image to Image Translation for Domain Adaptation. In: Proc. IEEE International Conference on Computer Vision and Pattern Recognition (CVPR), pp. 4500 – 4509 (2018)
42. NIST: NBIS- NIST Biometric Image Software. <http://biometrics.idealtest.org/>
43. Pathak, D., Krahenbuhl, P., Donahue, J., Darrell, T., Efros, A.A.: Context Encoders: Feature Learning by Inpainting. In: Proc. IEEE International Conference on Computer Vision and Pattern Recognition (CVPR), pp. 2536 – 2544 (2016)
44. Puri, C., Narang, K., Tiwari, A., Vatsa, M., Singh, R.: On Analysis of Rural and Urban Indian Fingerprint Images. In: Proc. International Conference on Ethics and Policy of Biometrics, pp. 55 – 61 (2010)
45. Qian, P., Li, A., Liu, M.: Latent Fingerprint Enhancement Based on DenseUNet. In: Proc. International Conference on Biometrics (ICB), pp. 1 – 6 (2019)
46. Qu, Z., Liu, J., Liu, Y., Guan, Q., Yang, C., Zhang, Y.: Orienet: A Regression System for Latent Fingerprint Orientation Field Extraction. In: Proc. International Conference on Artificial Neural Networks, pp. 436 – 446 (2018)
47. Rama, R.K., Namboodiri, A.M.: Fingerprint Enhancement using Hierarchical Markov Random Fields. In: Proc. IEEE International Joint Conference on Biometrics (IJCB), pp. 1 – 8 (2011)
48. Sahasrabudhe, M., Namboodiri, A.M.: Fingerprint Enhancement using Unsupervised Hierarchical Feature Learning. In: Proc. IAPR- and ACM-sponsored Indian Conference on Computer Vision, Graphics and Image Processing (ICVGIP), pp. 1 – 8 (2014)
49. Sankaran, A., Vatsa, M., Singh, R.: Multisensor Optical and Latent Fingerprint Database. IEEE Access **3**, 653 – 665 (2015)
50. Sankaranarayanan, S., Balaji, Y., Castillo, C.D., Chellappa, R.: Generate to Adapt: Aligning Domains using Generative Adversarial Networks. In: Proc. IEEE International Conference on Computer Vision and Pattern Recognition (CVPR), pp. 8503 – 8512 (2018)
51. Schuch, P., Schulz, S., Busch, C.: De-Convolutional Auto-encoder for Enhancement of Fingerprint Samples. In: Proc. International Conference on Image Processing Theory, Tools and Applications (IPTA), pp. 1 – 7 (2016)
52. Schuch, P., Schulz, S., Busch, C.: Survey on the Impact of Fingerprint Image Enhancement. IET Biometrics pp. 102 – 115 (2017)
53. Sharma, R.P., Dey, S.: Two-Stage Quality Adaptive Fingerprint Image Enhancement using Fuzzy C-Means Clustering Based Fingerprint Quality Analysis. Image and Vision Computing pp. 1 – 16 (2019)
54. Singh, K., Kapoor, R., Nayar, R.: Fingerprint denoising using ridge orientation based clustered dictionaries. Neurocomputing **167**, 418 – 423 (2015)
55. Svoboda, J., Monti, F., Bronstein, M.M.: Generative Convolutional Networks for Latent Fingerprint Reconstruction. In: Proc. IEEE International Joint Conference on Biometrics (IJCB), pp. 429 – 436 (2017)
56. Tiwari, K., Gupta, P.: Fingerprint Quality of Rural Population and Impact of Multiple Scanners on Recognition. In: Chinese Conference on Biometric Recognition, pp. 199 – 207 (2014)
57. Tzeng, E., Hoffman, J., Darrell, T., Saenko, K.: Simultaneous Deep Transfer Across Domains and Tasks. In: Proc. IEEE International Conference on Computer Vision and Pattern Recognition (CVPR), pp. 4068 – 4076 (2015)
58. Tzeng, E., Hoffman, J., Saenko, K., Darrell, T.: Adversarial Discriminative Domain Adaptation. In: Proc. IEEE International Conference on Computer Vision and Pattern Recognition (CVPR), pp. 7167 – 7176 (2017)
59. Tzeng, E., Hoffman, J., Zhang, N., Saenko, K., Darrell, T.: Deep Domain Confusion: Maximizing for Domain Invariance. arXiv preprint arXiv:1412.3474 (2014)
60. Vatsa, M., Singh, R., Bharadwaj, S., Bhatt, H., Mashruwala, R.: Analyzing Fingerprints of Indian Population Using Image Quality: A UIDAI Case Study. In: Proc. International Workshop on Emerging Techniques and Challenges for Hand-Based Biometrics, pp. 1 – 5 (2010)
61. Volpi, R., Morerio, P., Savarese, S., Murino, V.: Adversarial Feature Augmentation for Unsupervised Domain Adaptation. In: Proc. IEEE International Conference on Computer Vision and Pattern Recognition (CVPR), pp. 5495 – 5504 (2018)

-
- 62. Wang, W., Li, J., Huang, F., Feng, H.: Design and Implementation of Log-Gabor Filter in Fingerprint Image Enhancement. *Pattern Recognition Letters* **29**(3), 301 – 308 (2008)
 - 63. Wilson, G., Cook, D.J.: A Survey of Unsupervised Deep Domain Adaptation. *ACM Transactions on Intelligent Systems and Technology* **11**(5), 1 – 46 (2020)
 - 64. Wong, W.J., Lai, S.H.: Multi-Task CNN for Restoring Corrupted Fingerprint Images. *Pattern Recognition* **101**, 107203 – 107213 (2020)
 - 65. Yan, H., Ding, Y., Li, P., Wang, Q., Xu, Y., Zuo, W.: Mind the Class Weight Bias: Weighted maximum mean discrepancy for unsupervised domain adaptation. In: Proc. IEEE International Conference on Computer Vision and Pattern Recognition (CVPR), pp. 2272 – 2281 (2017)
 - 66. Yang, X., Feng, J., Zhou, J.: Localized Dictionaries Based Orientation Field Estimation for Latent Fingerprints. *IEEE Transactions on Pattern Analysis and Machine Intelligence* **36**(5), 955 – 969 (2014)
 - 67. Zhang, W., Xu, D., Ouyang, W., Li, W.: Self-Paced Collaborative and Adversarial Network for Unsupervised Domain Adaptation. *IEEE Transactions on Pattern Analysis and Machine Intelligence* **43**(6), 2047 – 2061 (2019)
 - 68. Zhu, J.Y., Park, T., Isola, P., Efros, A.A.: Unpaired Image-to-Image Translation using Cycle-Consistent Adversarial Networks. In: Proc. IEEE International Conference on Computer Vision (ICCV), pp. 2223 – 2232 (2017)